Synthesis of Double Hydrophilic Block Copolymers Poly(2-isopropyl-2-oxazoline- b -ethylenimine) and their DNA Transfection Efficiency

Gwendoline Delecourt, Laetitia Plet, Yann Le Guen, Ozgul Tezgel, Guillaume Tresset, Patrick Midoux, Tristan Montier, Véronique Bennevault, Philippe Guégan

Synthesis of Double hydrophilic block copolymers poly(2-isopropyl-2-oxazoline-*b*-ethylenimine) and their DNA transfection efficiency

Gwendoline Delecourt[1], Laetitia Plet[1], Yann Le Guen[2], Ozgul Tezgel[3], Guillaume Tresset[3], Patrick Midoux[4], Tristan Montier[2,5], Véronique Bennevault[1,6], Philippe Guégan[1,*]

[1] Institut Parisien de Chimie Moléculaire, Equipe Chimie des Polymères, UMR 8232 CNRS, Sorbonne University, 75252 Paris Cedex 05, France

[2] Univ Brest, INSERM, EFS, UMR 1078, GGB – GTCA team, 29200 Brest, France

[3] University of Paris-Saclay, CNRS, Laboratoire de Physique des Solides, 91405 Orsay, France

[4] Centre de Biophysique Moléculaire, CNRS UPR4301, 45071 Orléans Cedex 2, France

[5] CHRU de Brest, Service de Génétique Médicale et de Biologie de la Reproduction, Centre de Référence des Maladies Rares “Maladies Neuromusculaires”, 29200 Brest, France

[6] University of Evry, 91025 Evry Cedex, France

Keywords: PEI, gene therapy, PEGylation alternative, Oxazoline Keywords: ((3–7 keywords, not capitalized, plural, separated by commas, no full stop))

Abstract: ((Abstract text. 12 point, double-spaced. Maximum length 200 words. Written in the present tense.))

Gene delivery is now a part of our therapeutic arsenal. Various applications have been developed in the field of vaccination, inherited or acquired diseases treatments. Polymer synthetic vectors represent an opportunity to develop new treatments, with a prerequisite of improved delivery and reduced toxicity compared to existing polymers. We report the synthesis of linear poly(ethylenimine-*b*-2-isopropyl-2-oxazoline) block copolymers in a two step procedure with various molar masses of the linear polyethylenimine (*l*PEI) block. The molar mass of the poly(2-isopropyl-2-oxazoline) (PiPrOx) block is set to 7 kg.mol^{-1}. Condensation of plasmid DNA is successfully achieved, and in vitro transfection efficiency of

the copolymers is at least comparable to the one measured with the *l*PEI of same molar mass. The lPEI-*b*-piPrOx block copolymers are however less cytotoxic than their linear counterparts. The PiPrOx could be a good substituent to the PEG often used in drug delivery systems. The grafting of histidine moieties on the *l*PEI block of the *l*PEI-*b*-PiPrOx do not provide any real improvement of the gene delivery. A poor condensation of the pDNA is observed, probably due to increased steric hindrance along the *l*PEI backbone. The low cytotoxicity of the linear *l*PEI-*b*-PiPrOx family makes of this family a very good candidate for future developments in the gene delivery field.

1. Introduction

Gene transfer and its clinical application, gene therapy, constitute a major pathway for the development of future therapeutics based on nucleic acids (NA) targeting diseases that are beyond the reach of traditional pharmacological approaches.[1,2] Researches conducted for more than 30 years led to more than 3000 clinical trials,[3] and six products have now been approved and used in clinics.[4] Beyond gene therapy, the transfer of nucleic acids is also necessary for vaccination or for the production of CAR T cells or IPSCs**.** The gene delivery remains one of the utmost challenge and various vectors have been suggested to solve this issue with various pro and con. Today viral vectors are the most efficient gene carriers, however they suffer from various drawbacks including their potential for insertional mutagenesis,[5] immune response[6] and high production cost. Non-viral vectors allow to circumvent some of these shortcomings but they mostly suffer from poor transfection efficiency, suggesting for the requirement of new vectors for gene delivery applications. RNA-based vaccine against COVID19 were recently promoted, compared to viral one, thanks to their re-administration possibility associated to the need of intermediate expression required for this application. Considering non-viral gene delivery, polyethylenimine (PEI) is defined as the gold standard polymer since its used by Boussif et *al*.[7–9] Due to the positive charges along the polymer backbone,

complexation with the negatively charged NA permits to formulate nanoparticles called polyplexes. Therefore, NA is protected against nuclease degradation with limited induction of inflammation and immune responses.[10] Different structures and architectures of PEI can be reached depending on the synthetic pathway. *In vitro* studies carried out to date demonstrate a benefit of the linear polyethylenimine (*l*PEI) in comparison to the branched PEI (*b*PEI).[11,12] Nevertheless, the low transfection efficiency and the high toxicity of PEI-based vectors inhibited further development for human applications and suggested to go further.[13,14]. Accordingly, PEI–functionalization was undertaken to improve the transfection efficiency and to reduce the toxicity.[13,15] One common way to reduce the toxicity of polyplexes is to improve their stealthiness. Typically, the grafting of hydrophilic chains such as polyethylene glycol (PEG) allows the formation of polyplexes with smaller size, lower zeta potential and improved cell viability.[16–19] Furthermore, the polyplexes resulting from the grafting of PEG oligomers to linear cationic polymers allowed the reduction of immunogenicity,[20] and reduced hemolysis.[21] However, PEGylation limitations have been largely debated,[22–25] and alternative hydrophilic polymers are considered to replace it.[26–28] Biocompatibility of poly(2-alkyl-2-oxazoline)s (POx) has abundantly been discussed recently and application of POx as shielding shell in the formation of vectors for gene delivery is now the focus of many researches[29–31]. Then, PEI-POx copolymers synthesis by partial hydrolysis of POx homopolymers has been described,[32–34] leading to the formation of statistical copolymers PEI-*stat*-POx with a distribution of both repeating units (neutral and cationic) all along the macromolecular skeleton.[24] Other authors report double hydrophilic block copolymers by POx homopolymers grafting on PEI were obtained, that led to statistical and uncontrolled functionalization of the PEI backbone.[35,36] These seminal studies revealed the difficulty to obtained well-defined POx-*b*-PEI, enabling the formation of PEI-based polyplexes with a neutral hydrophilic POx shell surrounding the polyplex. To overcome the synthesis limitation, we previously developed a two-steps synthesis procedure leading to block copolymers of poly(2-oxazoline-*b*-

ethyleminine) (POx-*b*-PEI).[37] In the present work, we report the formulation of linear POx-*b*-PEI copolymers with pDNA to form polyplexes. Effects of copolymer molar masses and polymer/DNA weight ratio (WR) on transfection efficiency are investigated. POx-*b*-PEI copolymers are then functionalized by histidine derivatives in order to enhance endosomal escape of the polyplexes, as previously reported by Bertrand *et al*.[38], in order to avoid lysosomal enzymes. The physico-chemical parameters and *in vitro* transfection performances are analyzed in order to determine the best polymer and polyplexes formulation to enhance transfection efficiency with low toxicity.

2. Results and Discussion

2.1. Poly(2-alkyl-2-oxazoline)s

Previous works discussed the biocompatibility of POx homopolymers.[39] In order to confirm that our synthetic pathway enable to obtain non-cytotoxic polymers, a library of homopolymers of oxazoline was synthesized and their cytotoxicity compared to the one of PEG as a control was investigated using MTT assay.

2.1.1. Homopolymer synthesis

The polymerization of different oxazoline monomers (2-methyl-2-oxazoline, 2-ethyl-2-oxazoline, 2-isopropyl-2-oxazoline) was performed by cationic ring opening polymerization (CROP) initiated by allyl bromide as already reported (scheme 1).[40–42] All the polymerizations were carried out in acetonitrile at 80 °C with a constant monomer concentration ([Ox] = 1.5 mol.L^{-1}). The experimental conditions and analytical data are summarized in Table 1. The NMR and SEC molar masses are given after purification. For PEG, purification of the commercial product was performed by precipitation in diethyl ether after solubilization in methylene chloride.

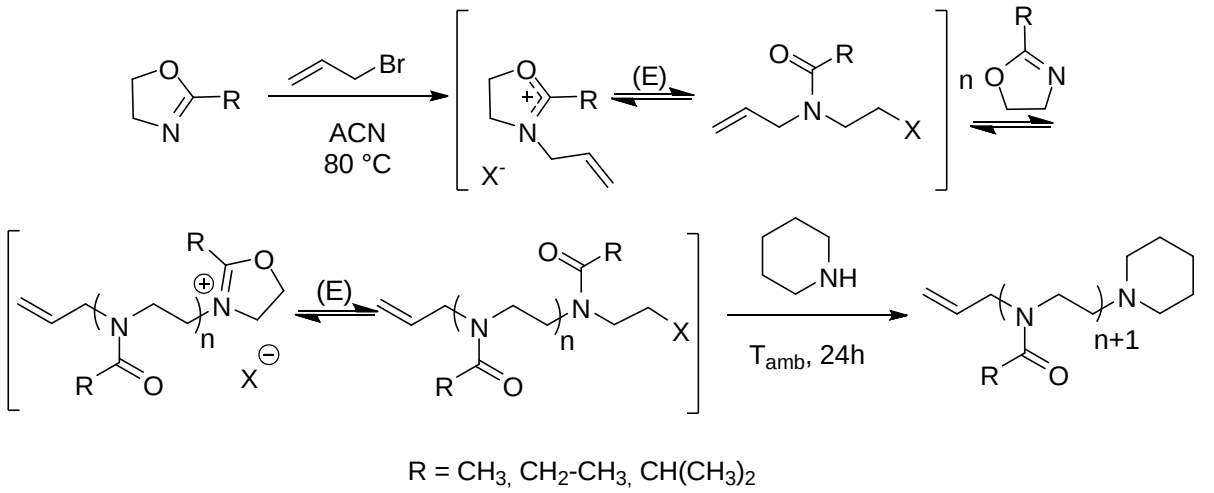

Scheme 1. Synthesis of homopolymers of 2-alkyl-2-oxazoline

Table 1. Characteristics of polyethylene glycol and homopolymers of 2-alkyl-2-oxazoline.

Polymers	Ox/I/Q[1]	Time[2] (h)	*p*[3] %	DPn (th)	M_n g.mol^{-1} (th)[4]	M_n g.mol^{-1} (RMN)[5]	M_n g.mol^{-1} (SEC)[6]	*Đ* (SEC)[6]
PEG	-	-	-	114[$]	-	4000	7600	1.04
PMeOx	58/1/10	42	100	58[#]	5000	5500	4800	1.18
PEtOx	50/1/10	72	97.2	51[#]	4900	5400	6500	1.10
PiPrOx	51/1/10	96	80	41[#]	4600	5600	7000	1.06

[$]DPn (th) gived by Sigma Aldrich; [#]DPn (th) = (([Ox]$_0$×*p*)/[I]$_0$; [1]I and Q correspond respectively to the initiator and quencher; [2]Polymerization time; [3]Ox conversions determined by ^{1}H NMR; [4]*M*n (th) = (([Ox]$_0$× M_{Ox} × *p*)/[I]$_0$; [5]determined by ^{1}H NMR; [6] determined by SEC in DMF, PMMA standards.

^{1}H NMR spectrum of PMeOx after purification is given as an example in Figure S1. The signal of the polymer backbone of Ox (methylene protons 4 and 5) appeared at 3.36 ppm. The methyl protons of the different 2-alkyl-2-oxazoline units give signals at 2.02 ppm for the PMeOx (protons 10) and at 1.05 ppm for PEtOx and PiPrOx. ^{1}H NMR analysis of the reaction medium at the end of the polymerization allows the determination of the conversion by comparison of the signal of the monomer methylene protons in the 3.6-4.0 ppm area and the one of the polymer backbone methylene protons at 3.36 ppm. The initiator alkene protons

(protons 1 and 2) were observed between 5.0 and 6.0 ppm and were used to determine the polymer molar mass (M_n NMR). The three homopolymers PMeOx, PEtOx and PiPrOx have NMR molar masses between 5400 and 5600 g.mol^{-1} in agreement with the theoretical values. The molar masses of each polymer were determined by DMF SEC. Obtained molar masses are closed to the NMR and theoretical values. The observed slight difference is due to the PMMA calibration.

2.1.2. Cytotoxicity tests

The polymer cytotoxicity was determined by performing MTT assay after 24h of treatment with different concentrations of polymer on HeLa and A549 cells (human epithelial cancerous cells). Results were presented in Figure 1.

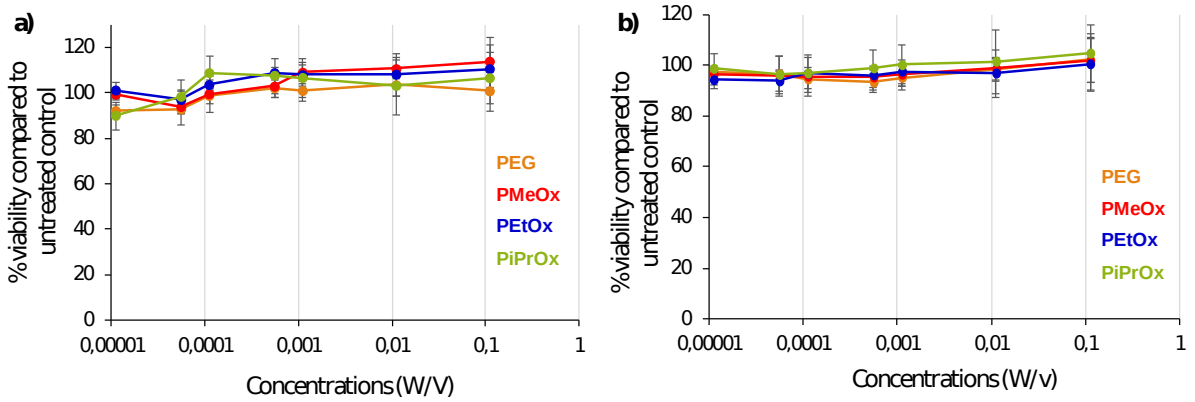

Figure 1. Viability of (a) Hela and (b) A459 cells. Cells were exposed to PEG and POx at different concentrations from 1.1×10^{-5} to 0.11 W/V. The cell viability was evaluated by MTT assay 24h after exposition and expressed as percentage relative of untreated cells.

Cell viability in the presence of PEG or one of the three poly(2-alkyl-2-oxazoline)s was determined as a function of polymer concentration. For all tested polymers, the cell viability was close to 100%, even at high concentration (0.11 W/V). The more hydrophobic PiPrOx

also presents very good cell viability. To conclude, these original POx have same biocompatibility as the PEG, in accordance to the literature,[39] therefore validating their use in the design of gene delivery cargo.

2.2. PEI-based polymers

Following the cell viability results, the synthesis of a PEI-*b*-PiPrOx copolymers library, and their derivatives, was carried out to further formulate polyplexes with a reporter pDNA in order to perform *in vitro* gene transfer experiments.

2.2.1. Polymer Synthesis

The library of (co)polymers (PEI abbreviated Px and PEI-*b*-PiPrOx abbreviated Cx) was obtained by hydrolyzing poly(2-methyl-2-oxazoline)s or selectively hydrolyzing poly(2-methyl-2-oxazoline-*b*-2-isopropyl-2-oxazoline)s according to previous work[37,42] (Table 2). L-histidine-N-acryloyl (HNA) residues, synthesized by addition elimination reaction of N-acryloyl on L-Histidine, were then grafted on the PEI backbone by Michael addition in order to functionalize polymers (Scheme 2).[38] Indeed, as described by Bertrand et *al*.,[38] histidine residues on PEI polymers enhance DNA transfection while reducing cytotoxicity. The "proton sponge" effect disrupts the endosome and facilitate the pDNA release into the cytosol. The pDNA copies have then to reach the nucleus to be expressed.[43] Finally, polymers Px-his and Cx-his were obtained.

Table 2. Polymers characteristics**.**

PEI-based polymers					Histidinylated polymers			
Run[a]	Polymer type	M_n PEI [kg.mol^{-1}]	M_n PiPrOx [kg.mol^{-1}]	EI mass content[d] [%]	Run[b]	Polymer type	EI modified[c] [%]	EI mass content[d] [%]
P1	PEI	15	-	100	P1-his	PEI(his)	11.5	62
P2		10	-	100	P2-his		12.8	59
P3		5	-	100	P3-his		8.1	70
C1	PEI-*b*-PiPrOx	15	5.7	72	C1-his	PEI(his)-*b*-PiPrOx	18.7	42
C2		10	5.7	63	-		-	-
C3		5	5.7	47	-		-	-

[a]Px: homopolymer of polyethylenimine; Cx: copolymer PEI-*b*-PiPrOx; [b]Px-his, Cx-his: polymers functionalized by histidine moieties on ethylenimine units, [c]% of EI units

functionalized by HNA, [d] percentage by mass of EI units in the polymer (EI mass content = EI mass / polymer mass, more details in Table S1)

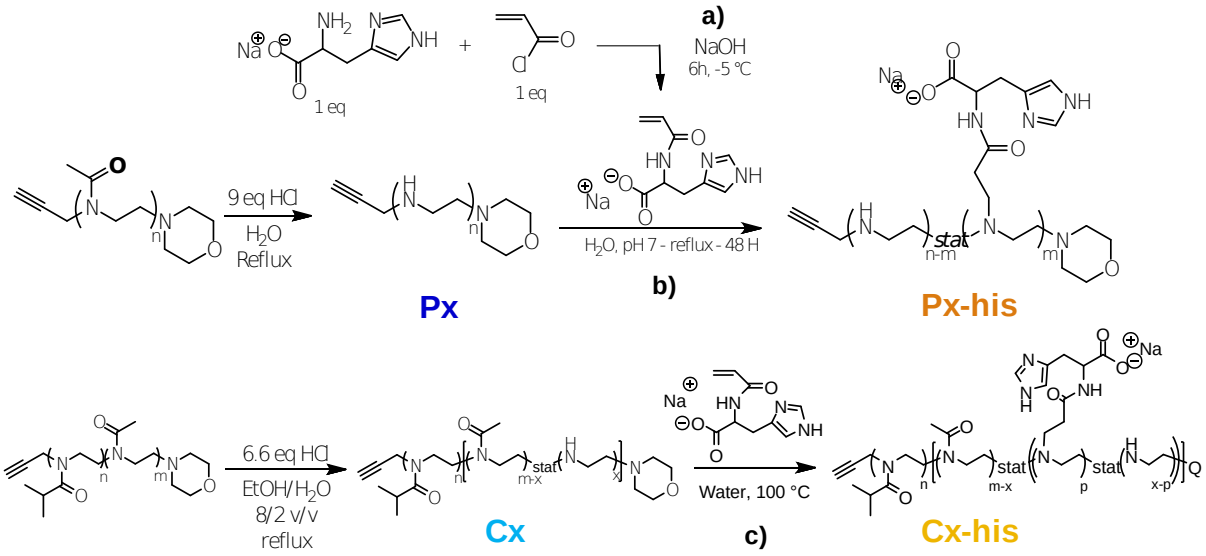

Scheme 2: Synthesis of (a) L-Histidine-N-acryloyl (HNA) by addition elimination reaction, and functionalization of (b) homopolymers Px and (c) copolymers Cx by HNA by Michael addition to obtain Px-his and Cx-his.

The library of polymers is divided into PEI-based polymers with homopolymers Px from 5 to 15 kg.mol^{-1} and their counterpart copolymers Cx with PEI block from 5 to 15 kg.mol^{-1} and PiPrOx block of 5.7 kg.mol^{-1}.

These different polymers were functionalized with L-Histidine-*N*-acryloyl to obtained Px-his and Cx-his. The %EI modified represent the percentage of EI units functionalized by HNA. For Px, all the polymers were functionalized and Px-his were obtained with 8.1 to 12.8 % of EI modified. For Cx, the functionalization is more difficult due to the poor solubility of the polymer at high temperature. Only C1 was modified with success in EtOH and reflux. 18.7% of EI units were functionalized by HNA (C1-his). ^{1}H NMR spectrum of P1-his was presented in Figure S2.

2.2.2 Formulation and characterization of polyplexes.

Polyplexes formulation consisted in a fast mixing of a synthetic cationic (co)polymer Px or Cx solution poured into the plasmid (pTG11033) solution at different weight ratio (WR) polymer/pDNA as previously described in literature.[44] First, *l*PEI and *l*PEI-*b*-PiPrOx are studied, and the formulation parameters (concentrations and volumes) are presented in Table S1. Polyplexes Px/pDNA and Cx/pDNA obtained are named respectively P(Px) and P(Cx).

Physico-chemical parameters of obtained complexes are studied by electrophoresis in order to determine the optimal weight ratios for efficient DNA complexation, and by DLS as the size and zeta potential of the polyplexes are known to affect the transfection and cytotoxicity performances. For this study, two different weight ratios were considered. The ratio WR was calculated considering the mass of polymer (WRpolymer = mass of polymer / mass of DNA), while the ratio WRPEI took in account only the mass of PEI contained in the polymer (WRPEI = mass of polymer × %PEI / mass of DNA)

Electrophoresis shift assays:

Polyplexes were analyzed by electrophoretic mobility shift assay (EMSA). Electrophoretic separation was performed on polyplexes P(Px) and P(Cx) in an agarose gel was presented in Figure 2. The influence of the (co)polymer structure and the weight ratio used on their capacity to condensate the pDNA was investigated.

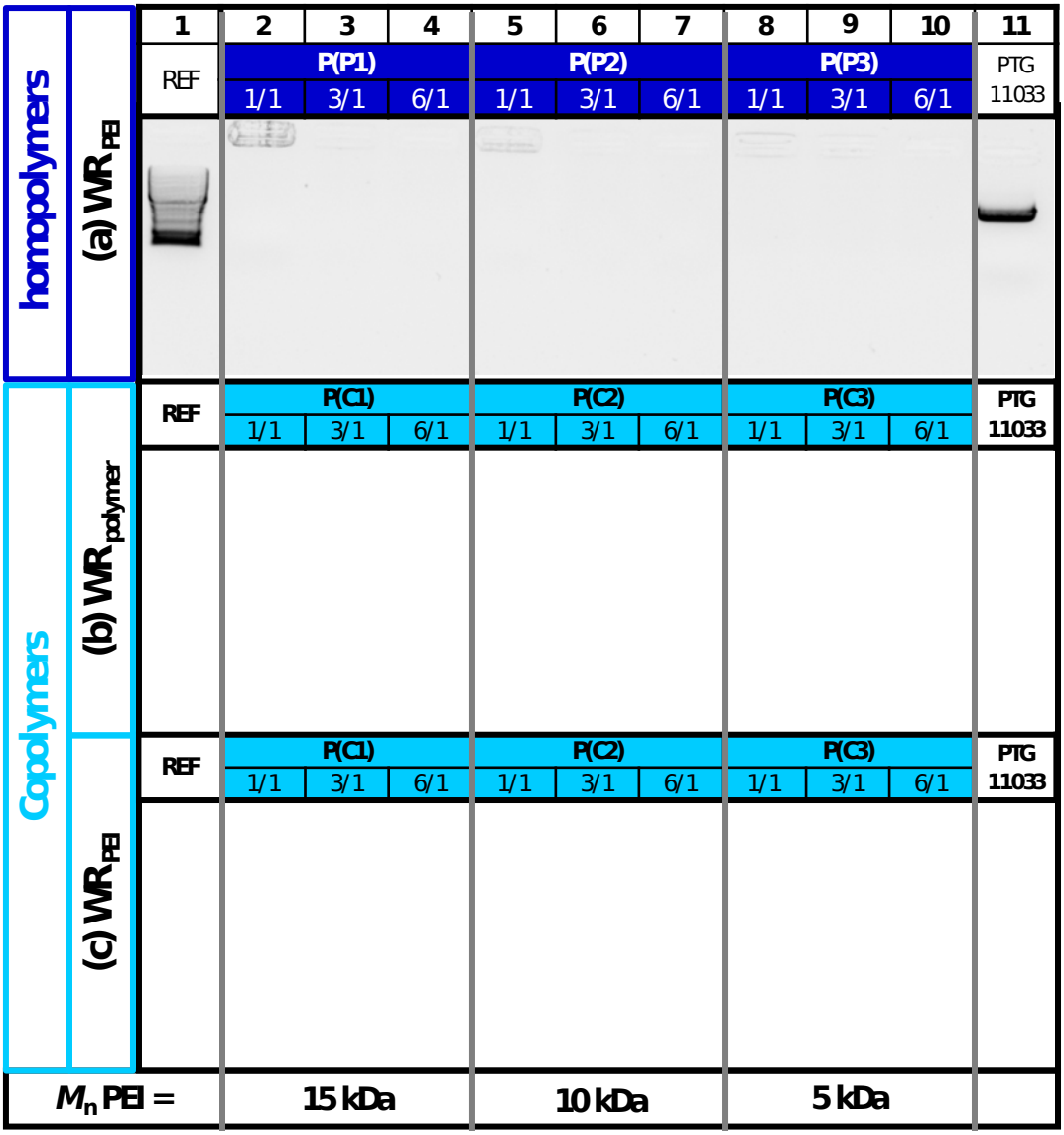

Figure 2. Electrophoretic mobility shift essay. Polyplexes (0.5 µg DNA equivalent) were loaded in a 0.6% agarose gel and electrophoresis and run for 30 min at 120 V in TAE. Lane 1: molecular-weight size markers, lanes 2 to 10: polyplexes formed with (a) homopolymers *l*PEI or (b and c) copolymers PEI-*b*-PiPrOx with different molar masses at different WR ($WR_{polymer}$ or WR_{PEI} = 1/1, 3/1, 6/1); lane 11: pDNA alone.

For P(Px) complexes obtained with PEI, no migration is observed at the different WRs and molar masses tested: the complexes formed are the result of efficient condensation of pDNA with an increasing efficiency with the WR increasing. Indeed, the fluorescence observed from wells is decreasing from WR 1/1 to WR 6/1 for the three polymer molar masses.

Concerning the PEI-*b*-PiPrOx copolymers, two series of formulations have been performed using either $WR_{polymer}$ or WR_{PEI} (calculations details in Table S1). Better pDNA condensation

was observed with WR_{PEI}. DNA condensation was similar for P(C1) and P(C2) polyplexes at the 3 WR_{PEI} tested. For C3-based complexes, a diffuse migration was observed at WR_{PEI} 1/1, suggesting a less effective condensation. In comparison, its PEI counterpart, P(P3), showed efficient complexation of the plasmid at this same WR, demonstrating that even a 5 kDA linear PEI is sufficient to achieve this condensation. Thus, in the case of the corresponding copolymer, the PiPrOx block limited the complexation of the pDNA by the PEI block. It was then necessary to increase the amount of copolymer to fully complex the pDNA. To conclude, all the (co)polymers used allowed the pDNA complexation.

This analysis also highlighted that it was relevant to use WR_{PEI} weight ratio instead of $WR_{polymer}$ to compare the copolymers to their PEI counterparts for pDNA condensation performances. It was then anticipated that the same conclusion held for biological studies, so only WR_{PEI} 3/1 and 6/1 will be used for the following assays because they presented better condensation efficiency.

Size and zeta potential:

Size and surface charge of P(Px) and P(Cx) complexes were analyzed using DLS and zeta potential measurement respectively. Results were reported in Figures 3 and 4.

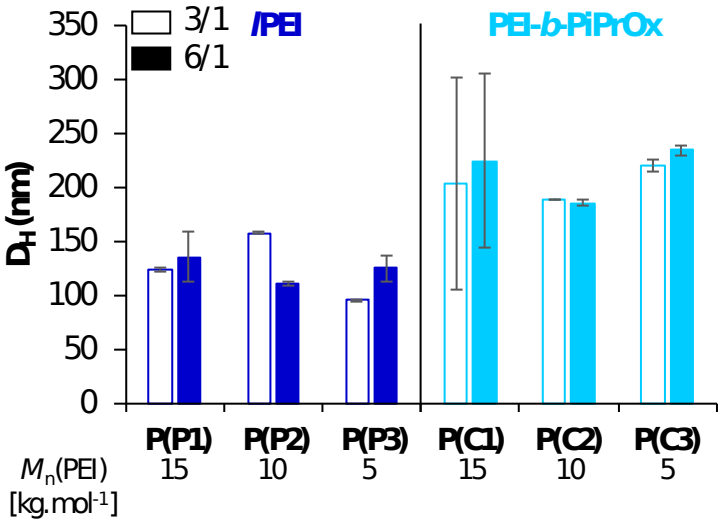

Figure 3. Hydrodynamic diameters of polyplexes obtained with WR_{PEI} 3/1 and 6/1. (DLS: Horiba, 25 °C). Standard deviations are from 3 successive measurements with the same sample.

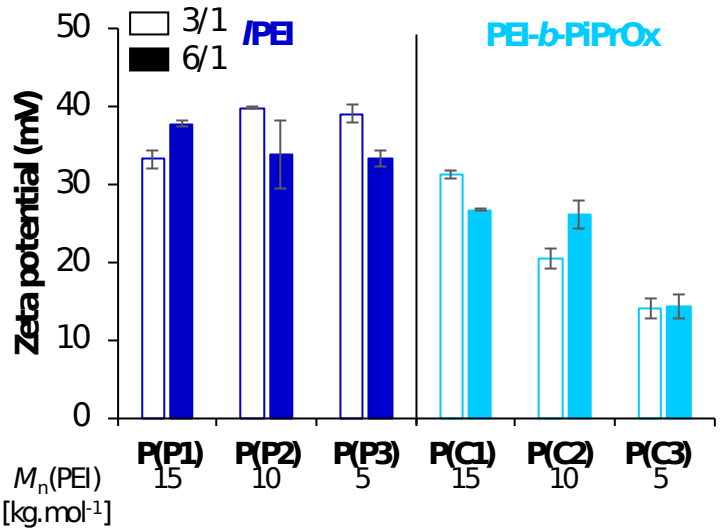

Figure 4. Zeta potential of polyplexes obtained with WR_{PEI} 3/1 and 6/1. (DLS: Horiba, 25°C). Standard deviations are from 3 successive measurements with the same sample.

The complexes sizes range from 100 to 235 nm (Figure 3). Homopolymer-based complexes, P(Px), have a size between 100 and 158 nm while copolymers ones, P(Cx), have a size between 190 and 235 nm and PDI below 0.3. The addition of the PiPrOx block on the polymer increased the size of the polyplexes. Furthermore, as expected, the addition of the POx block on the polymer vector reduced the surface charge of the polyplexes: 40 mV for P(Px) compared to 30 to 15 mV for P(Cx)'s. These analyses appeared to demonstrate that the PiPrOx block was located around the pDNA/PEI core forming a hydrophilic shell. The partly charged surface could be attributed to the presence of cationic polymer or to the solvation of the PiPrOx block by water as previously observed for other polymers.[27] The addition of the hydrophilic block therefore had an impact on the internal organization of the complex. This was demonstrated by Cryo-TEM analysis (Figure 5).

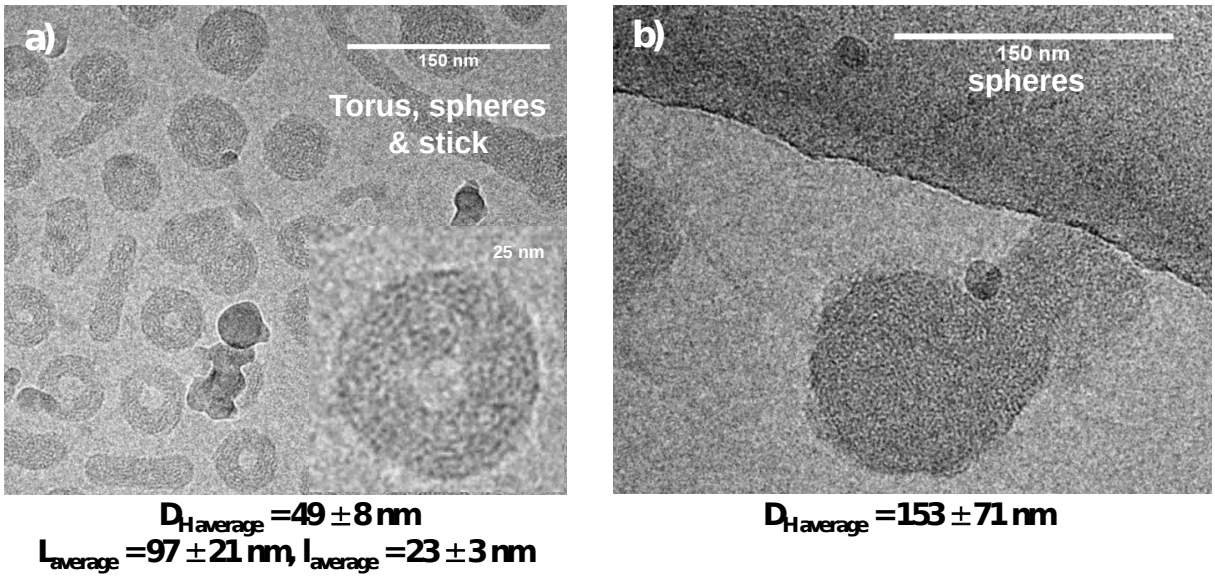

Figure 5. Cryo-TEM pictures of polyplexes obtained with (a) P1 and (b) C2.

P1-based complexes are organized in tores and rods. The objects have a size of 49 ± 8 nm of diameter for tores and 97 ± 21 nm × 23 ± 3 nm for rods. Futhermore, as previously observed with these polymers,[43] an internal organization can be observed by the presence of white "streaks" and testifies for a strong pDNA/polymer interaction. The complexes are therefore very stable. In the case of complexes formulated with copolymer C2, a single population of globular spherical objects was observed (see also Figure S3). There was no longer any organization in the form of torus or rods. Moreover, the internal organization was less visible and complexes of larger diameter were observed in comparison with *l*PEI P1. These different observations were related to the addition of the hydrophilic block PiPrOx and confirmed the hypothesis of a different organization made previously during the study of complexe size.

Polyplexes stability:

To evaluate the pDNA release into the cytosol during transfection experiments, the complex stability was studied. Complexes P(Px) and P(Cx) were incubated during 30 min with different amounts of dextran sulfate, which is a complexation competitor to pDNA. Electrophoretic mobility assays were then performed and the pDNA release was quantified

using ImageJ (details are presented in Figure S4) and analyzed as a function of the dextran sulfate quantity (Figure 6).

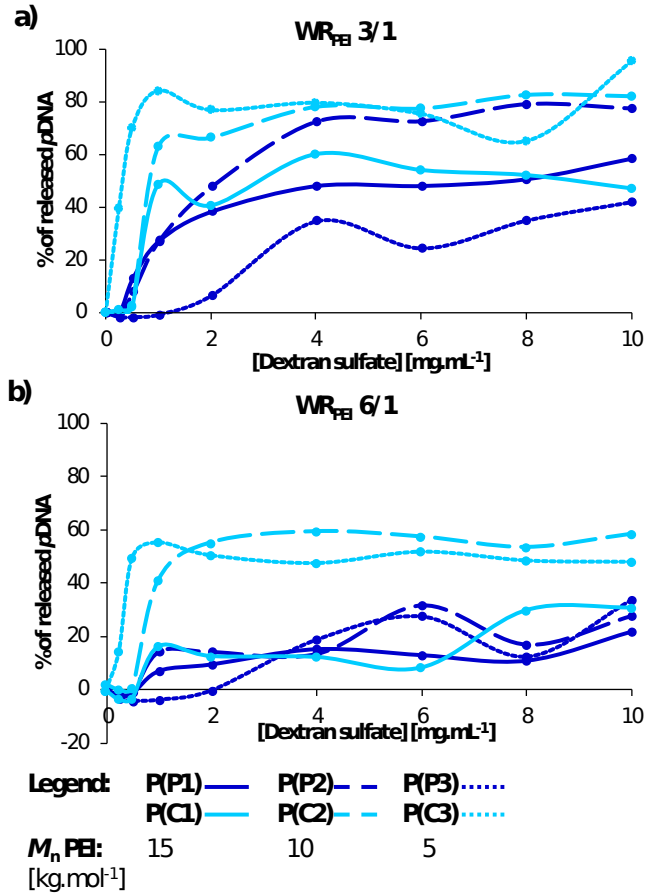

Figure 6. Percentage of released pDNA in function of the dextran sulfate concentration for homopolymers *l*PEI (Px) and copolymers PEI-*b*-PiPrOx (Cx) with WR_{PEI} (a) 3/1 and (b) 6/1.

For all the analyzed complexes, one led to a fast released of pDNA, followed by a plateau that demonstrates it did not exist a total pDNA release. Some pDNA remained complexed whatever the added amount of dextran, suggesting the presence of polyplexes with high cohesive energy, and plateaus depended on the nature of the (co)polymer used to form the polyplexes. For P(Px) at WR_{PEI} 3/1, the plateau was reached at a dextran sulfate concentration of 4 $mg.mL^{-1}$ with the decomplexation of 30% to 75 % of pDNA depending on the molar mass of the polymer. In comparison, at the same WR with the copolymers, the plateau was reached with a lower concentration of dextran sulfate (1 $mg.mL^{-1}$) with a decomplexation ranging from 50 % to 95 % of pDNA, meaning that copolymer-based complexes were slightly less

stable than the homopolymer-based polyplexes regarding the competitive complexation of dextran sulfate.

For the WR_{PEI} 6/1, a similar observation can be done: copolymer-based complexes were less stable than the ones formulated with homopolymers since the plateaus were reached at lower concentration of sulfate dextran (0.5-1 $mg.mL^{-1}$ for P(Cx) and 1-2 $mg.mL^{-1}$ for P(Px)). Nevertheless, at this WR_{PEI}, around 60 % and 20% of decomplexation was observed for P(Cx) and P(Px) respectively. Complexes were more stable in comparison with WR_{PEI} 3/1.

This very high cohesive energy highlighted here was a well-known phenomenon for linear PEI-based complexes. Indeed, Maury et *al*.[43] demonstrated by electronic microscopy an internal structuring of the complexes for *l*PEI, that was lost when the *l*PEI was derivatized by histidine residue, for example. This was also shown by DeRouchey et *al*.[45] by decomplexation experiments in the presence of NaCl. The complexes exposed to an increasing concentration of NaCl and analyzed by SAXS showed a very good stability allowed by the hexagonal structure of the complexes. Nevertheless, a too high cohesive energy could be detrimental to the transfection efficacy because the complex must be able to dissociate in the cytosol to release the pDNA and allow the plasmid expression.

On the other hand, the copolymers molar masses have an impact on the stability: an augmentation of the PEI block molar mass allowed to enhance the complexes stability. Few pDNA was released at a same sulfate dextan concentration for both WR_{PEI} using long PEI block. For example, at a WR_{PEI} 3/1 with sulfate dextran concentration of 1 $mg.mL^{-1}$, 85%, 65% and 50 % of pDNA were released using a PEI block of 5, 10 and 15 kDa respectively. P(C1) must be highlighted as the pDNA decomplexation was very similar to the homopolymer counterparts, P(P1), suggesting a similar cohesive energy between P(C1) and P(P1). To conclude, the use of copolymers tends to reduce the cohesive energy of the polyplexes, suggesting a higher tendency for pDNA release in the cytoplasm during

transfection experiments. The modulation of the molar mass of the *l*PEI block of the copolymers enabled the balancing of the cohesive energy of the polyplexes.

2.2.3 *In vitro* analyses

The effective complexation properties of pDNA by the (co)polymer library allowed to consider transfection experiments, and cytotoxicity of Px- and Cx-based complexes with Mn_{PEI} of 15, 10 and 5 kDa with WR_{PEI} 3/1 and 6/1.

Cytotoxicity tests:

The cytotoxicity of polymers Px and Cx was tested by MTT assays on HepG2 cells (Figure 7).

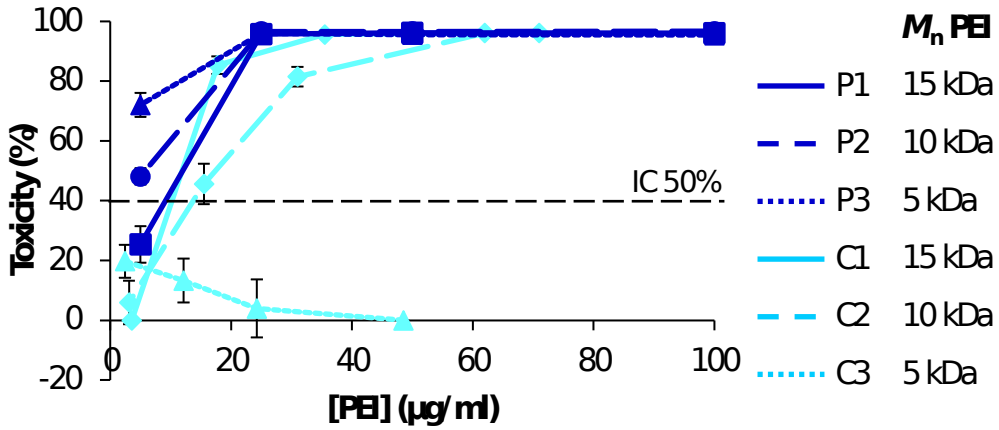

Figure 7. Cytotoxicity of homopolymers PEI (Px) and copolymers PEI-*b*-PiPrOx (Cx) on HepG2 cells as function of the PEI concentration.

First, with Px, an increased cytotoxicity appeared when decreasing the molar mass of the polymer used to formulate the pDNA. This was not in agreement with the literature which described an increased cytotoxicity with increasing molar mass.[14] However, the IC50% are respectively 5 and 10 µg.mL^{-1} for P2 and P1. These values were in the same range as those of Bertrand *et al.*[38] with other cells lines.

Copolymers PEI-*b*-PiPrOx exhibited a lower cytotoxicity than their homopolymer counterparts. For the same molar mass of PEI, Cx were less cytotoxic than Px. This was more

pronounced with C3 that was not toxic at any concentration used (0 to 50 µg.mL^{-1}). With C2 the IC50% is 18 µg.mL^{-1}, while it was 5 µg.mL^{-1} with P2. C1 and P1 exhibited the same IC50% of 10 µg.mL^{-1}. Regarding the copolymer results, the ratio Mn_{PEI}/Mn_{PiPrOx} can be related to the cytotoxicity: higher the ratio was, higher the cytotoxicity was. Reducing the molar mass of PEI block (decrease of the ratio) led to have better biocompatibility of the polymer. This was in accordance with the biocompatibily of PiPrOx.

Transfection efficiency:

Transfection efficiency of P(Px) and P(Cx) was evaluated on HepG2 cells after 4h of exposition of the cells to the polyplexes solution and 48h of culture in the absence of polyplexes. Figure 8 presented the results with WR_{PEI} of 3/1 and 6/1.

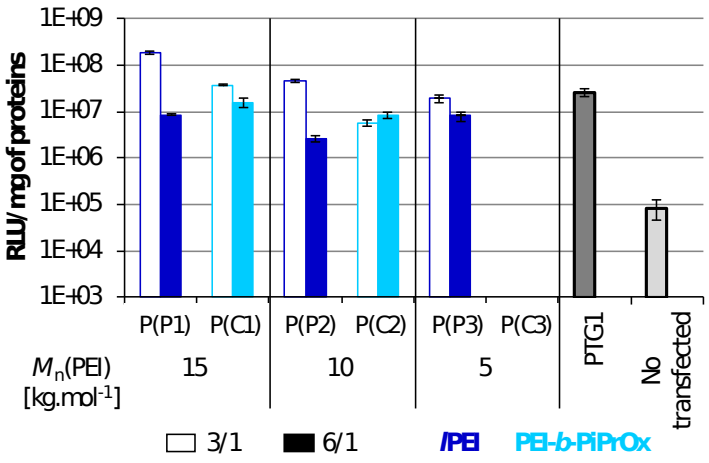

Figure 8. Transfection efficiency of polyplexes. HepG2 cells were transfected for 4 h with polyplexes of *l*PEI (P(Px)) and PEI-*b*-PiPrOx (P(Cx)) containing 2.5 µg of *p*TG11033 with WR_{PEI} 3/1 and 6/1. The luciferase activity was expressed as relative light unit (RLU) per mg protein after 48 h. The values showed average of three independent experiments. (PTG1: commercial reference from Polytheragene®).

For each type of polyplexes (P(Px) and P(Cx)), a slight decrease of the transfection efficiency was observed with the diminution of PEI block molar mass. All polyplexes (excepted P(C3)) exhibited a transfection efficiency close to the commercial reference PTG1. P(C3) did not

allow transfection although the polymer demonstrated very low cytotoxicity (Figure 7). This could be explained by the low zeta potential of polyplexes (Figure 4) that decreased their interactions with cells and reduced the uptake and their low stability (Figure 6) that could lead to polyplexes disruption before their endocytosis or too rapidly once inside the cells.

For P(C1) and P(C2), results were interesting as the transfection efficiency was very close to P(P1) and P(P2). At WR_{PEI} 6/1, the efficiency was even better for P(C1) and P(C2) in comparison with P(P1) and P(P2) respectively. The addition of the PiPrOx block did not affect the efficiency of the transfection.

These results showed that the copolymer PEI-*b*-PiPrOx 10-5.7 $kg.mol^{-1}$ (C2) combined efficient pDNA complexation, high stability, low cytotoxicity and efficient transfection of polyplexes exhibiting a size of 190 nm and a zeta potential of 20-25 mV.

2.2.2. Evaluation of histidine functionalization of the block copolymers

The last part of this study concerned the biological benefit of histidine residues on copolymers. Bertrand et *al*.[38] demonstrated that His-*l*PEI was expected to be a promising carrier for non-viral gene transfer due to its very low cytotoxicity and good transfection efficiency. Therefore, the synthesis of PEI(his)-*b*-PiPrOx and their PEI(his) counterpart was performed (Table 2). The pDNA complexation, cytotoxicity and the transfection efficiency of polyplexes were then studied.

Polymers P1-his and C1-his (Table 2) were used to produce the corresponding complexes P(P1-his) and P(C1-his) at different $WR_{PEI.}$

Electrophoresis shift essays:

To characterize the pDNA complexation, P(P1-his) and P(C1-his) formulated at different WR_{PEI} are analyzed by electrophoresis shift essay (Figure 9).

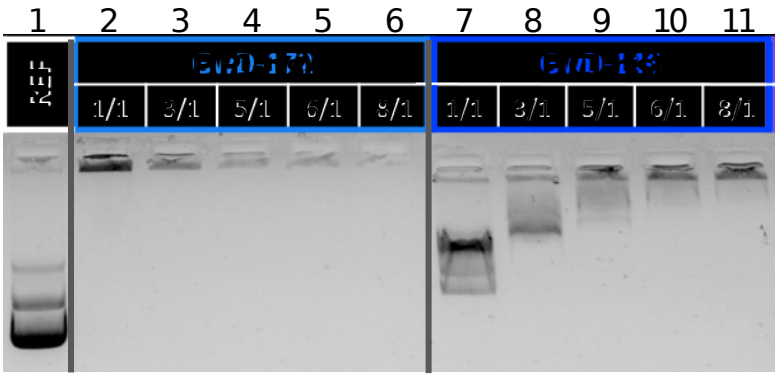

Figure 9. Electrophoretic mobility shift assay. Polyplexes (0.5 µg DNA) were loaded in a 0.6% agarose gel and electrophoresis and run for 30 min at 120 V in TAE. Lane 1: pDNA; lanes 2 to 11: polyplexes formed with histidinylated *l*PEI (P1-his) and copolymer PEI-*b*-PiPrOx (C1-his) at different WR_{PEI} (1/1, 3/1, 5/1, 6/1, 8/1).

For complexes formed with P(P1-his), no migration was observed whatever the WR_{PEI} used. P(P1-his) demonstrated efficient pDNA condensation for all WR_{PEI} tested as for *l*PEI.

For P(C1-his), the pDNA condensation was less strong: migration of pDNA was observed for WR_{PEI} of 1/1 to 5/1. WR_{PEI} of 6/1 and 8/1 led to complete pDNA condensation but the fluorescence signal is high indicating that the dye can intercalate in the DNA proving a weaker DNA condensation with P(C1-his) than with P1-his. Same explanation as for the P(P1-his) compared to P(P1) can be given: HNA functionalization induced steric hindrance and decrease in the cohesive energy. Furthermore, PiPrOx block had a negative impact on condensation as observed previously for P(Cx) (Figure 2). Indeed, in P(C1-his), 40 % of the polymer mass corresponded to histidine moieties and 16 % were PiPrOx block. 44 % of the polymer remained as PEI units. The pDNA condensation was, therefore, less dense and less efficient.

To perform *in vitro* tests, WR_{PEI} 3/1 and 6/1 were selected as before to permit comparison between functionalized and unfunctionalized polymers although P(P1-his) showed less effective condensation with WR_{PEI} 3/1. Again, cytotoxicity analysis was performed before transfection essays to validate the (co)polymer choice.

Cytotoxicity tests:

The cytotoxicity of complexes P(P1-his) and P(C1-his) at WR_{PEI} 3/1 and 6/1 was tested by MTT assays on HepG2 cells (Figure 10) and compared to the cytotoxicity of PTG1 and P(C1) used previously.

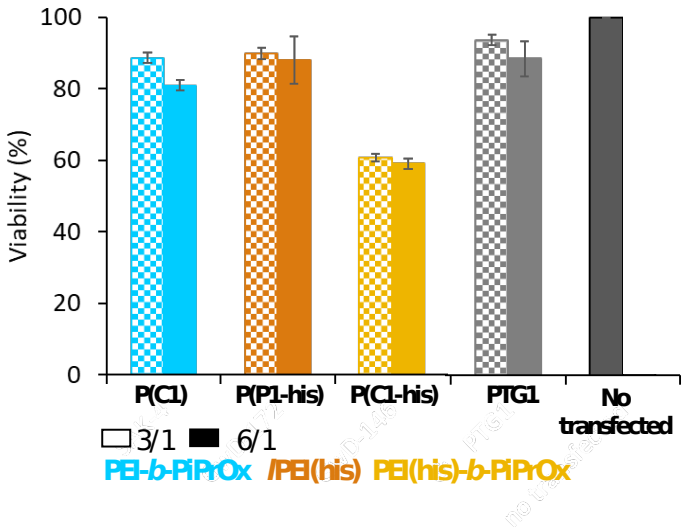

Figure 10. HepG2 cell viability with polyplexes obtained with copolymers without or with histidinylation (C1 and C1-his respectively) and histidinylated homopolymers PEI (P1-his) with PEI block of 15 $kg.mol^{-1}$ at WR_{PEI} 3/1 and 6/1. (PTG1: commercial reference from Polytheragene®)

Low toxicity was observed for P(P1-his)-based formulations for the tested WR_{PEI}. They were closed to the toxicity of the commercial product (< 10%). Surprisingly, P(C1-his)-based polyplexes had a higher toxicity than the P(C1): 40 % cells death was obtained for both WR_{PEI} used. The poor complexation of DNA by this polymer, as shown in the electrophoretic analyses, suggested higher number of free polymer chains responsible for the toxicity. For both polyplexes tested (P(P1-his) and P(C1-his), a slight toxicity increase was observed at WR_{PEI} 6/1, probably related to the higher number of free chains in solution.[46]

Transfection efficiency:

As previously mentioned, histidine functionalization led to improve transfection by enhancing the endosome release. Thus, transfection efficiency of P(C1), P(P1-his) and P(C1-his) was evaluated and the results were gathered in Figure 11.

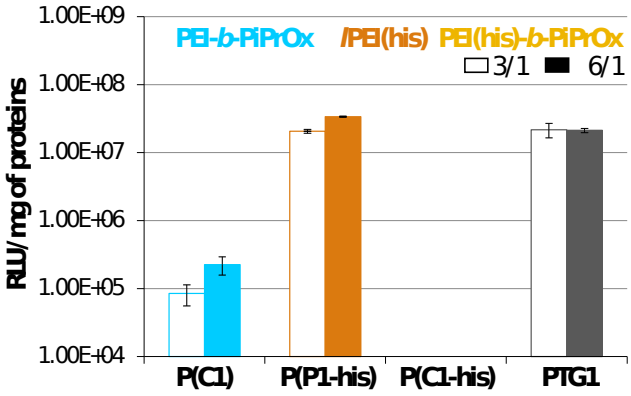

Figure 11. Transfection efficiency of polyplexes formulated. HepG2 cells were transfected for 4 h with polyplexes of PEI-*b*-PiPrOx (C1), PEI-his (P1-his) and PEI(his)-*b*-PiPrOx (C2-his) containing 1 µg of *p*TG11033 with WR_{PEI} 3/1 and 6/1. The luciferase activity was measured after 48 h of culture and was expressed as relative light unit (RLU) per mg protein. The values shown average of three independent experiments. (PTG1: commercial reference from Polytheragene®)

The polyplexes obtained with the homopolymers functionalized by histidine (P(P1-his)) exhibited same tranfection efficiency as the reference. Nevertheless, the same functionalization on copolymers (P(C1-his)) did not lead to any gene expression at all. This negative result was explained by the weaker pDNA condensation illustrated in Figure 9.

To conclude on the HNA functionalization, the transfection efficiency of the polyplexes obtained with the functionalized polymer P1-his was again promising. Nevertheless, the HNA functionalization of PEI in the copolymer did not provide positive effect.

3. Conclusion

Copolymers PEI-*b*-PiPrOx with different PEI block molar masses and their PEI counterparts were synthetized. Their complexation with pDNA was analyzed in terms of size, zeta potential, complexation and stability to choose better conditions to perform *in vitro* transfection essays. Complexes P(Px) and P(Cx) with WR_{PEI} of 3/1 and 6/1 were found to be the best candidates for *in vitro* transfection essays. Cytotoxicity tests demonstrated the advantages of the hydrophilic and biocompatible PiPrOx block as the toxicity was reduced with copolymers compare to homopolymers. Nevertheless, to obtain good transfection efficiency, it was necessary to use PEI block of 15 or 10 $kg.mol^{-1}$ at least, ascertaining the requirement for large molar mass of PEI blocks in gene delivery applications. Combining all the results, PEI-*b*-PiPrOx 10-5.7 $kg.mol^{-1}$ met the initial requirements: polyplexes presenting good pDNA condensation with size around 190 nm, reduced cytotoxicity compared to *l*PEI homopolymers and the transfection efficiency was preserved. In order to combine stealthiness functionalization with an enhanced endosomal escape, copolymer C1 was functionalized by histidine but the poor pDNA condensation at the WR tested did not lead to improve *in vitro* transfection results. This functionalization has to be improved notably by grafting a lower number of histidine residues to reduce steric hindrance.

4. Experimental Section

Materials**:** *p*TG11033 (9514 bp) was purchased from Tebu-bio (Le Perray-en-Yvelines, France). Linear PEI, histidinylated PEI, copolymers PEI-*b*-PiPrOx were synthesized as described.[37,38,42]. The histidinylated copolymers PEI(his)-*b*-PiPrOx were synthesized with adaptation of the procedure used for PEI (details below). Acetonitrile (CH_3CN, VWR), allyl bromide (99%, Aldrich), 2-ethyl-2-oxazoline (99%, Aldrich), 2-methyl-2-oxazoline (98%, Aldrich), and 2-isopropyl-2-oxazoline (97%, TCI) were purified by refluxing over calcium hydride under nitrogen and distilled prior to use. Piperidine (99%, Aldrich) was dried over molecular sieves (3 Å) activated by heating at 150°C overnight under vacuum prior to use.

Hepes, NaOH, HCl (37%) were purchased from Aldrich (St. Quentin Fallavier, France) (Solution of 10 mM Hepes was prepared in distilled water). Nuclepore Track-etched membranes were purchased from Merck. Eagle's mini-mum essential medium (MEM), foetal bovine serum (FBS), penicillin-streptomycin solution (penicillin 10.000 $IU.mL^{-1}$ and streptomycin 10 $mg.mL^{-1}$), the phosphate buffered saline (PBS) came from PAA Laboratories, Les Mureaux, France. Agarose was from Lonza (Bâle, Swiss).

***Instrumentation*:**

Size and zeta potential : Size polyplexes were measured in 10 mM HEPES buffer, pH 7.4 at 25°C by dynamic light scattering (DLS) with SZ-100 Nanopartica from Horiba (Les Ulis, France). Samples were illuminated with a 10 mW laser at 532 nm. The light scattering was measured at 90° for the size and at 13° for the zeta potential.

***Methods*:**

Poly(2-alkyl-2-oxazoline) homopolymers synthesis: Polymerization of MeOx, EtOx, iPrOx was conducted in acetonitrile at 80°C in a 100 mL schlenk flask degassed under high vacuum and flamed out. The following procedure of polymerization is detailed for PMeOx.

A 1.5 M solution of 2-methyl-2-oxazoline (4 mL, $4.72.10^{-2}$ $mol.L^{-1}$, 58 eq) in acetonitrile (27.5 mL) with allyl bromide (70 µL, $8.09.10^{-4}$ mol, 1 eq) was stirred at 80°C under N_2 atmosphere. After complete conversion of MeOx (42 h), the shlenck was cooled down to room temperature. An excess of piperidine (800 µL, $8.09.10^{-3}$ mol, 10 eq) was added to quench the reaction and stirred all night long. ^{1}H NMR spectroscopy analysis of the reaction medium was performed to ascertain MeOx conversion. Then, the solvent was evaporated and the polymer was dried in vacuum overnight at 50°C and purified by two dialyses against ACN, for the first one, and water, for the second one. The polymer was recovered by freeze drying. The synthesized polymer was analysed by SEC and NMR spectroscopy in order to determine M_n and $Đ$ and to confirm its structure.

Quantities and monomer/initiator ratios used for the other polymerizations were summarized in the Table 1 in the manuscript.

Copolymers synthesis: The diblock poly(2-isopropyl-2-oxazoline-*b*-2-methyl-2-oxazoline)s were synthesized via cationic ring-opening polymerization of oxazolines by sequential monomer additions, then the copolymers are selectively hydrolyzed to conduct to double hydrophilic block copolymers poly(2-isopropyl-2-oxazoline-*b*-ethylenimine)s according a procedure described by Delecourt et *al.*[37].

Homopolymers functionalization by L-Histidine-N-acryloyl: The functionalization of PEI by L-histidine-*N*-acryloyl was performed by Michael addition according a procedure described by Bertrand et *al.*[38]

Copolymers functionalization by L-Histidine-N-acryloyl: The functionalization of PEI-*b*-PiPrOx by L-histidine-*N*-acryloyl was performed by Michael addition based on the procedure described by Bertrand et *al.*[38] The functionalization is performed in ethanol at reflux with 0,6 eq/EI unit of HNA and 0,6 eq/EI unit of DIPEA during 2 days.

Polyplexes formulation: Polyplexes were prepared with different weight ratio polymer/pDNA (WR) in Hepes 10 mM (pH 7.4). The appropriated quantity of polymer (solution at 0.5 $mg.mL^{-1}$ or at 5 $mg.mL^{-1}$) was added quickly drop by drop to a pDNA solution at 0.0714 $\mu g.mL^{-1}$ or 0.714 $\mu g.mL^{-1}$ with vortex stirring. Volumes of each solution are indicated in respective Tables.

Electrophoretic mobility shift assays: Free pDNA and polyplexes were analyzed on a 0.6% agarose gel. Gel running buffer was TAE (Tris base, acetic acid and EDTA) and pDNA gel was stained with Sybr safe (solution diluted 20000x). The migration was running for 30 min at 120 V.

Cells and cell culture: Human hepatoma cells (HepG2, 8055 HB; ATCC, Rockville, MD, USA) were cultured at 37°C under 5% CO_2 in DMEM containing 10% heat-inactivated fetal bovine serum (FBS), 2 mM l-glutamine, 100 $Units.ml^{-1}$ penicillin, and 50 $Units.ml^{-1}$

streptomycin. Cells were harvested once a week in PBS containing 1 $mg.mL^{-1}$ trypsin and 5 mM EDTA.

Cervical adenocarcinoma epithelial cells (HeLa), and alveolar adenocarcinoma epithelial cells (A549) were cultured in DMEM containing 10% heat-inactivated fetal bovine serum, 1% antibiotics (10,000 U mL-1 Penicillin, 10,000 µg mL-1 Streptomycin), and 1% L-Glutamine. These lines were maintained in a humid atmosphere at 37°C, 5% CO2. Regular maintenance was performed.

Transfection assays: 24-well plates were seeded with cells at 1.5×10^5 cells/well in 1 mL of culture medium. After 24 h of culture, the medium was discarded and cells were incubated during 4 h at 37°C with polyplexes (1 µg of DNA/well) in 500 µL of cell culture medium with 10 % of FBS. Then, the medium containing polyplexes was discarded and replaced by 1 mL of standard culture medium (10 % of FBS no decomplemented, 0.4 % of penicillin and streptomycin and 1 % of glutamax). After 48 h, the luciferase activity in cell lysate was measured with a luciferase dosage kit (Promega, E1500) and a luminometer (LUMAT LB 9507). The luciferase activity was normalized by the total quantity of proteins measured by the BCA protein dosage (Uptima, Interchim SA, Montuçon, France) and was expressed in relative luminescent unit (RLU) per mg of protein. For one polyplexe type given, the transfection was performed in triplicate.

Cytotoxicity assays: 24-well plates were seeded with cells at $1.5.10^5$ cells/well in 0.9 mL of culture medium. After 24 h of culture, 100 µL of polymer solutions in Hepes 10 mM, pH 7.4 were added (all concentrations were tested in triplicate). After 48 h, 3-(4,5-dimethylthiazol-2-yl)-2,5-diphenyltetrazolium bromide (MTT; 100 µl of 5 $mg.mL^{-1}$ solution in PBS, yellow color) was added in culture wells. After 4 h incubation at 37°C, the culture medium was discarded and the formazan synthetized was solubilized by adding acidic isopropanol (HCl at $3.6.10^{-2}$ $mol.L^{-1}$) and 200 µL of sodium dodecylsulfate (SDS) at 3% in water. After 30 min incubating at ambient temperature, 200 µL were collected and added in triplicate in a 96-well

plate (as 3 wells of the 24-well plate represent the same concentration, the cytotoxicity was calculated with 9 well in the 96-well plate). The absorbance at 570 nm was measured with Victor I spectrophotometer and cytotoxicity expressed as a percentage of absorbance relative to control cells (cells without any treatments).

Cryotransmission electron microscopy. A holey carbon grid (Quantifoil R2/2, Germany) was ionized by glow discharge prior to the deposition of 4 µL of sample solution. The grid was plunged into liquid ethane cooled down by liquid nitrogen using a FEI Vitrobot cryoplunger (FEI, Oregon) with a blotting time of 1.5 s and a relative humidity of 100%. Samples stored in liquid nitrogen were transferred into a Gatan 626 cryoholder (Gatan, California) and imaged via a 200-kV field emission gun JEOL 2010F microscope (Japan). Images were collected at a magnification of ×50,000 using a minimal dose system with a Gatan Ultrascan 4K CCD camera. The nominal defocus was set between 2.0 and 3.0 µm.

Supporting Information ((delete if not applicable))
Supporting Information is available from the Wiley Online Library or from the author.

Acknowledgements

This work was supported by the Fondation pour la Recherche Médicale, France, grant number PLP20161036677 to Laetitia Plet and the Agence Nationale pour la Recherche, France (ANR-17-CE18-0015-01-VINP). The electron microscopy imaging is supported by "Investissements d'Avenir" LabEx PALM (contract ANR-10-LABX-0039-PALM) and by the program "Moyens de Recherche Mutalisés" of the Université Paris-Saclay. Association de Transfusion Sanguine et de Biogénétique Gaétan Saleün" (Brest, France), SFR SCINBIOS/IBSAM (Brest, France), "Conseil Régional de Bretagne" (France), and "Brest Métropole" (France)

Received: ((will be filled in by the editorial staff))
Revised: ((will be filled in by the editorial staff))
Published online: ((will be filled in by the editorial staff))

References

(1) Friedmann, T.; Roblin, R. Gene Therapy for Human Genetic Disease? *Science* **1972**, *175* (4025), 949–955. https://doi.org/10.1126/science.175.4025.949.
(2) Cring, M. R.; Sheffield, V. C. Gene Therapy and Gene Correction: Targets, Progress, and Challenges for Treating Human Diseases. *Gene Therapy* **2020**, 1–10. https://doi.org/10.1038/s41434-020-00197-8.

(3) Ginn, S. L.; Amaya, A. K.; Alexander, I. E.; Edelstein, M.; Abedi, M. R. Gene Therapy Clinical Trials Worldwide to 2017: An Update. *The Journal of Gene Medicine* **2018**, *20* (5), e3015. https://doi.org/10.1002/jgm.3015.
(4) High, K. A.; Roncarolo, M. G. Gene Therapy. *N Engl J Med* **2019**, *381* (5), 455–464. https://doi.org/10.1056/NEJMra1706910.
(5) Braun, C. J.; Boztug, K.; Paruzynski, A.; Witzel, M.; Schwarzer, A.; Rothe, M.; Modlich, U.; Beier, R.; Göhring, G.; Steinemann, D.; Fronza, R.; Ball, C. R.; Haemmerle, R.; Naundorf, S.; Kühlcke, K.; Rose, M.; Fraser, C.; Mathias, L.; Ferrari, R.; Abboud, M. R.; Al-Herz, W.; Kondratenko, I.; Maródi, L.; Glimm, H.; Schlegelberger, B.; Schambach, A.; Albert, M. H.; Schmidt, M.; von Kalle, C.; Klein, C. Gene Therapy for Wiskott-Aldrich Syndrome--Long-Term Efficacy and Genotoxicity. *Sci Transl Med* **2014**, *6* (227), 227ra33. https://doi.org/10.1126/scitranslmed.3007280.
(6) Dunbar, C. E.; High, K. A.; Joung, J. K.; Kohn, D. B.; Ozawa, K.; Sadelain, M. Gene Therapy Comes of Age. *Science* **2018**, *359* (6372), eaan4672. https://doi.org/10.1126/science.aan4672.
(7) Rai, R.; Alwani, S.; Badea, I. Polymeric Nanoparticles in Gene Therapy: New Avenues of Design and Optimization for Delivery Applications. *Polymers* **2019**, *11* (4), 745. https://doi.org/10.3390/polym11040745.
(8) Boussif, O.; Lezoualc'h, F.; Zanta, M. A.; Mergny, M. D.; Scherman, D.; Demeneix, B.; Behr, J. P. A Versatile Vector for Gene and Oligonucleotide Transfer into Cells in Culture and in Vivo: Polyethylenimine. *Proc. Natl. Acad. Sci. U.S.A.* **1995**, *92* (16), 7297–7301. https://doi.org/10.1073/pnas.92.16.7297.
(9) Demeneix, B.; Behr, J. Polyethylenimine (PEI). In *Advances in Genetics*; Non-Viral Vectors for Gene Therapy, Second Edition: Part 1; Academic Press, 2005; Vol. 53, pp 215–230. https://doi.org/10.1016/S0065-2660(05)53008-6.
(10) Pichon, C.; Billiet, L.; Midoux, P. Chemical Vectors for Gene Delivery: Uptake and Intracellular Trafficking. *Curr Opin Biotech* **2010**, *21* (5), 640–645. https://doi.org/10.1016/j.copbio.2010.07.003.
(11) Kafil, V.; Omidi, Y. Cytotoxic Impacts of Linear and Branched Polyethylenimine Nanostructures in A431 Cells. *Bioimpacts* **2011**, *1* (1), 23–30. https://doi.org/10.5681/bi.2011.004.
(12) Okon, E. U.; Hammed, G.; Wafa, P. A. E.; Abraham, O.; Case, N.; Henry, E. In-Vitro Cytotoxicity of Polyethyleneimine on HeLa and Vero Cells. *IJIAS* **2014**, *5* (3), 192–199.
(13) de Oliveira, F. A.; Albuquerque, L. J. C.; Delecourt, G.; Bennevault, V.; Guégan, P.; Giacomelli, F. C. Current Designs of Polymeric Platforms Towards the Delivery of Nucleic Acids Inside the Cells with Focus on Polyethylenimine. *Curr Gene Ther* **2021**, *21* (5), 431–451. https://doi.org/10.2174/1566523221666210705130238.
(14) Rinkenauer, A. C.; Vollrath, A.; Schallon, A.; Tauhardt, L.; Kempe, K.; Schubert, S.; Fischer, D.; Schubert, U. S. Parallel High-Throughput Screening of Polymer Vectors for Nonviral Gene Delivery: Evaluation of Structure–Property Relationships of Transfection. *ACS Comb. Sci.* **2013**, *15* (9), 475–482. https://doi.org/10.1021/co400025u.
(15) Jäger, M.; Schubert, S.; Ochrimenko, S.; Fischer, D.; Schubert, U. S. Branched and Linear Poly(Ethylene Imine)-Based Conjugates: Synthetic Modification, Characterization, and Application. *Chem. Soc. Rev.* **2012**, *41* (13), 4755–4767. https://doi.org/10.1039/C2CS35146C.
(16) Suk, J. S.; Xu, Q.; Kim, N.; Hanes, J.; Ensign, L. M. PEGylation as a Strategy for Improving Nanoparticle-Based Drug and Gene Delivery. *Adv. Drug Deliv. Rev.* **2016**, *99*, 28–51. https://doi.org/10.1016/j.addr.2015.09.012.
(17) Salameh, J. W.; Zhou, L.; Ward, S. M.; Chalarca, C. F. S.; Emrick, T.; Figueiredo, M. L. Polymer-Mediated Gene Therapy: Recent Advances and Merging of Delivery

Techniques. *WIRES Nanomed. nanobi.* **2020**, *12* (2), e1598. https://doi.org/10.1002/wnan.1598.
(18) Zhang, X.; Pan, S.-R.; Hu, H.-M.; Wu, G.-F.; Feng, M.; Zhang, W.; Luo, X. Poly(Ethylene Glycol)-Block-Polyethylenimine Copolymers as Carriers for Gene Delivery: Effects of PEG Molecular Weight and PEGylation Degree. *J. Biomed. Mater. Res. A* **2008**, *84A* (3), 795–804. https://doi.org/10.1002/jbm.a.31343.
(19) Brissault, B.; Kichler, A.; Leborgne, C.; Danos, O.; Cheradame, H.; Gau, J.; Auvray, L.; Guis, C. Synthesis, Characterization, and Gene Transfer Application of Poly(Ethylene Glycol-b-Ethylenimine) with High Molar Mass Polyamine Block. *Biomacromolecules* **2006**, *7* (10), 2863–2870. https://doi.org/10.1021/bm060499a.
(20) Uchida, S.; Itaka, K.; Chen, Q.; Osada, K.; Ishii, T.; Shibata, M.-A.; Harada-Shiba, M.; Kataoka, K. PEGylated Polyplex With Optimized PEG Shielding Enhances Gene Introduction in Lungs by Minimizing Inflammatory Responses. *Molecular Therapy* **2012**, *20* (6), 1196–1203. https://doi.org/10.1038/mt.2012.20.
(21) Neu, M.; Germershaus, O.; Béhé, M.; Kissel, T. Bioreversibly Crosslinked Polyplexes of PEI and High Molecular Weight PEG Show Extended Circulation Times in Vivo. *Journal of controlled release : official journal of the Controlled Release Society* **2007**. https://doi.org/10.1016/J.JCONREL.2007.08.009.
(22) Knop, K.; Hoogenboom, R.; Fischer, D.; Schubert, U. S. Poly(Ethylene Glycol) in Drug Delivery: Pros and Cons as Well as Potential Alternatives. *Angew. Chem. Int. Edit* **2010**, *49* (36), 6288–6308. https://doi.org/10.1002/anie.200902672.
(23) Zhang, P.; Sun, F.; Liu, S.; Jiang, S. Anti-PEG Antibodies in the Clinic: Current Issues and beyond PEGylation. *J. Control. Release* **2016**, *244*, 184–193. https://doi.org/10.1016/j.jconrel.2016.06.040.
(24) Ishida, T.; Kiwada, H. Accelerated Blood Clearance (ABC) Phenomenon upon Repeated Injection of PEGylated Liposomes. *Int J Pharm* **2008**, *354* (1–2), 56–62. https://doi.org/10.1016/j.ijpharm.2007.11.005.
(25) Yang, Q.; Lai, S. K. Anti-PEG Immunity: Emergence, Characteristics, and Unaddressed Questions. *WIRES Nanomed. nanobi.* **2015**, *7* (5), 655–677. https://doi.org/10.1002/wnan.1339.
(26) Abbina, S.; Parambath, A. 14 - PEGylation and Its Alternatives: A Summary. In *Engineering of Biomaterials for Drug Delivery Systems*; Parambath, A., Ed.; Woodhead Publishing Series in Biomaterials; Woodhead Publishing, 2018; pp 363–376. https://doi.org/10.1016/B978-0-08-101750-0.00014-3.
(27) Du, H.; de Oliveira, F. A.; Albuquerque, L. J. C.; Tresset, G.; Pavlova, E.; Huin, C.; Guégan, P.; Giacomelli, F. C. Polyglycidol-Stabilized Nanoparticles as a Promising Alternative to Nanoparticle PEGylation: Polymer Synthesis and Protein Fouling Considerations. *Langmuir* **2020**, *36* (5), 1266–1278. https://doi.org/10.1021/acs.langmuir.9b03687.
(28) Dentzer, L.; Bray, C.; Noinville, S.; Illy, N.; Guégan, P. Phosphazene-Promoted Metal-Free Ring-Opening Polymerization of 1,2-Epoxybutane Initiated by Secondary Amides. *Macromolecules* **2015**, *48* (21), 7755–7764. https://doi.org/10.1021/acs.macromol.5b01638.
(29) Bludau, H.; Czapar, A. E.; Pitek, A. S.; Shukla, S.; Jordan, R.; Steinmetz, N. F. POxylation as an Alternative Stealth Coating for Biomedical Applications. *Eur. Polym. J* **2017**, *88*, 679–688. https://doi.org/10.1016/j.eurpolymj.2016.10.041.
(30) Morgese, G.; Benetti, E. M. Polyoxazoline Biointerfaces by Surface Grafting. *Eur. Polym. J* **2017**, *88*, 470–485. https://doi.org/10.1016/j.eurpolymj.2016.11.003.
(31) Goddard, P.; Hutchinson, L. E.; Brown, J.; Brookman, L. J. Soluble Polymeric Carriers for Drug Delivery. Part 2. Preparation and in Vivo Behaviour of N-Acylethylenimine

Copolymers. *J. Control. Release* **1989**, *10* (1), 5–16. https://doi.org/10.1016/0168-3659(89)90013-8.
(32) de la Rosa, V. R.; Bauwens, E.; Monnery, B. D.; De Geest, B. G.; Hoogenboom, R. Fast and Accurate Partial Hydrolysis of Poly(2-Ethyl-2-Oxazoline) into Tailored Linear Polyethylenimine Copolymers. *Polym. Chem.* **2014**, *5* (17), 4957–4964. https://doi.org/10.1039/C4PY00355A.
(33) Fernandes, J. C.; Qiu, X.; Winnik, F. M.; Benderdour, M.; Zhang, X.; Dai, K.; Shi, Q. Linear Polyethylenimine Produced by Partial Acid Hydrolysis of Poly(2-Ethyl-2-Oxazoline) for DNA and SiRNA Delivery in Vitro. *Int J Nanomedicine* **2013**, *8*, 4091–4102. https://doi.org/10.2147/IJN.S47413.
(34) Kuringen, H. P. C. V.; Lenoir, J.; Adriaens, E.; Bender, J.; Geest, B. G. D.; Hoogenboom, R. Partial Hydrolysis of Poly(2-Ethyl-2-Oxazoline) and Potential Implications for Biomedical Applications? *Macromol. Biosci.* **2012**, *12* (8), 1114–1123. https://doi.org/10.1002/mabi.201200080.
(35) Hsiue, G.-H.; Chiang, H.-Z.; Wang, C.-H.; Juang, T.-M. Nonviral Gene Carriers Based on Diblock Copolymers of Poly(2-Ethyl-2-Oxazoline) and Linear Polyethylenimine. *Bioconjugate Chem.* **2006**, *17* (3), 781–786. https://doi.org/10.1021/bc050317u.
(36) Haladjova, E.; Halacheva, S.; Momekova, D.; Moskova-Doumanova, V.; Topouzova-Hristova, T.; Mladenova, K.; Doumanov, J.; Petrova, M.; Rangelov, S. Polyplex Particles Based on Comb-Like Polyethylenimine/Poly(2-Ethyl-2-Oxazoline) Copolymers: Relating Biological Performance with Morphology and Structure. *Macromol. Biosci.* **2018**, *18* (4), 1700349. https://doi.org/10.1002/mabi.201700349.
(37) Delecourt, G.; Plet, L.; Bennevault, V.; Guégan, P. Synthesis of Double Hydrophilic Block Copolymers Poly(2-Oxazoline-b-Ethylenimine) in a Two-Step Procedure. *ACS Appl. Polym. Mater.* **2020**, *2* (7), 2696–2705. https://doi.org/10.1021/acsapm.0c00308.
(38) Bertrand, E.; Gonçalves, C.; Billiet, L.; Gomez, J. P.; Pichon, C.; Cheradame, H.; Midoux, P.; Guégan, P. Histidinylated Linear PEI: A New Efficient Non-Toxic Polymer for Gene Transfer. *Chem. Commun. (Camb.)* **2011**, *47* (46), 12547–12549. https://doi.org/10.1039/c1cc15716g.
(39) Viegas, T. X.; Bentley, M. D.; Harris, J. M.; Fang, Z.; Yoon, K.; Dizman, B.; Weimer, R.; Mero, A.; Pasut, G.; Veronese, F. M. Polyoxazoline: Chemistry, Properties, and Applications in Drug Delivery. *Bioconjugate Chem.* **2011**, *22* (5), 976–986. https://doi.org/10.1021/bc200049d.
(40) Bennevault-Celton, V.; Urbach, A.; Martin, O.; Pichon, C.; Guégan, P.; Midoux, P. Supramolecular Assemblies of Histidinylated α-Cyclodextrin in the Presence of DNA Scaffold during CDplexes Formation. *Bioconjugate Chem.* **2011**, *22* (12), 2404–2414. https://doi.org/10.1021/bc200167p.
(41) Pereira, G.; Huin, C.; Morariu, S.; Bennevault-Celton, V.; Guégan, P. Synthesis of Poly(2-Methyl-2-Oxazoline) Star Polymers with a β-Cyclodextrin Core. *Australian Journal of Chemistry* **2012**, *65*, 1145. https://doi.org/10.1071/CH12232.
(42) Plet, L.; Delecourt, G.; Hanafi, M.; Pantoustier, N.; Pembouong, G.; Midoux, P.; Bennevault, V.; Guégan, P. Controlled Star Poly(2-Oxazoline)s: Synthesis, Characterization. *Eur. Polym. J* **2020**, *122*, 109323. https://doi.org/10.1016/j.eurpolymj.2019.109323.
(43) Maury, B.; Gonçalves, C.; Tresset, G.; Zeghal, M.; Cheradame, H.; Guégan, P.; Pichon, C.; Midoux, P. Influence of pDNA Availability on Transfection Efficiency of Polyplexes in Non-Proliferative Cells. *Biomaterials* **2014**, *35* (22), 5977–5985. https://doi.org/10.1016/j.biomaterials.2014.04.007.
(44) Brissault, B.; Kichler, A.; Guis, C.; Leborgne, C.; Danos, O.; Cheradame, H. Synthesis of Linear Polyethylenimine Derivatives for DNA Transfection. *Bioconjugate Chem.* **2003**, *14* (3), 581–587. https://doi.org/10.1021/bc0200529.

(45) DeRouchey, J.; Netz, R. R.; Rädler, J. O. Structural Investigations of DNA-Polycation Complexes. *Eur. Phys. J. E* **2005**, *16* (1), 17–28. https://doi.org/10.1140/epje/e2005-00003-4.
(46) Aravindan, L.; Bicknell, K. A.; Brooks, G.; Khutoryanskiy, V. V.; Williams, A. C. Effect of Acyl Chain Length on Transfection Efficiency and Toxicity of Polyethylenimine. *Int. J. Pharm.* **2009**, *378* (1), 201–210. https://doi.org/10.1016/j.ijpharm.2009.05.052.

The table of contents entry should be 50–60 words long and should be written in the present tense. The text should be different from the abstract text.

C. Author 2, D. E. F. Author 3, A. B. Corresponding Author* ((same order as byline))

Title ((no stars))

ToC figure ((Please choose one size: 55 mm broad × 50 mm high **or** 110 mm broad × 20 mm high. Please do not use any other dimensions))

Supporting Information

Synthesis of Double hydrophilic block copolymers poly(2-isopropyl-2-oxazoline-*b*-ethylenimine) and their DNA transfection efficiency

*Gwendoline Delecourt, Laetitia Plet, Yann Le Guen,Ozgül Tezgel, Guillaume Tresset, Patrick Midoux, Tristan Montier, Véronique Bennevault, Philippe Guégan**

Figure S1: ^{1}H NMR spectrum of PMeOx in $CDCl_3$

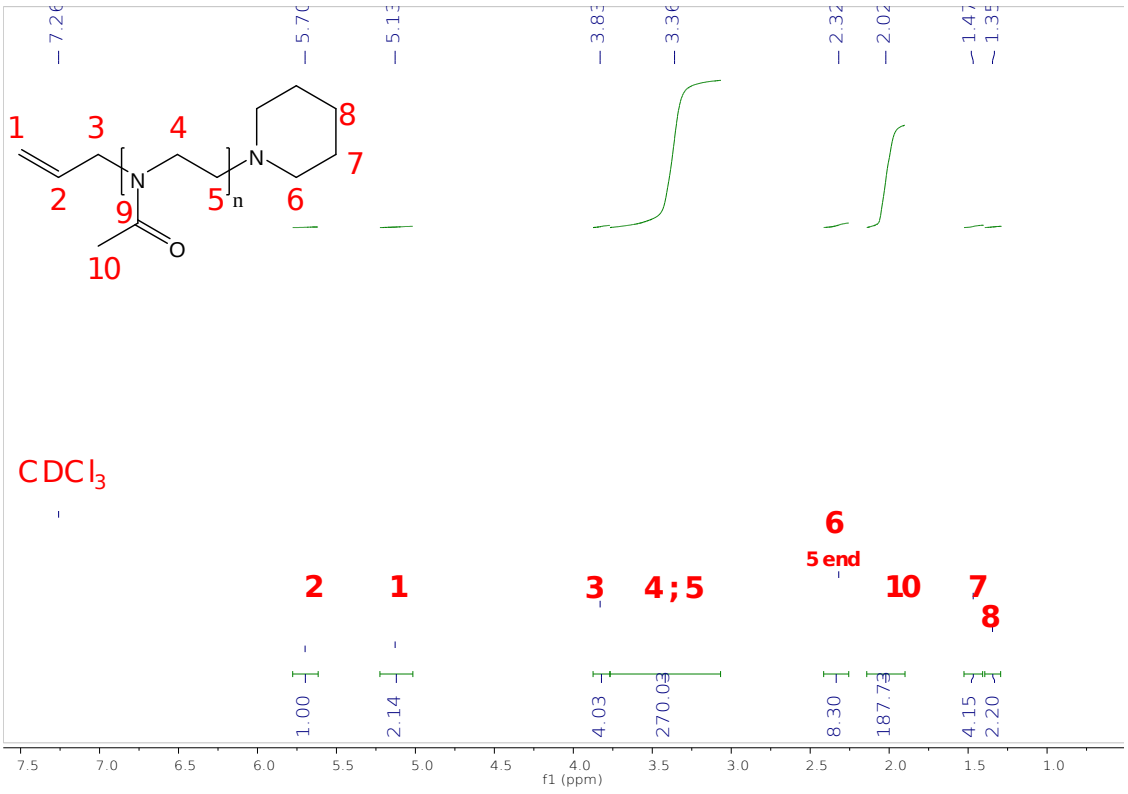

Figure S2: ^{1}H NMR spectrum of C1-his in D_2O

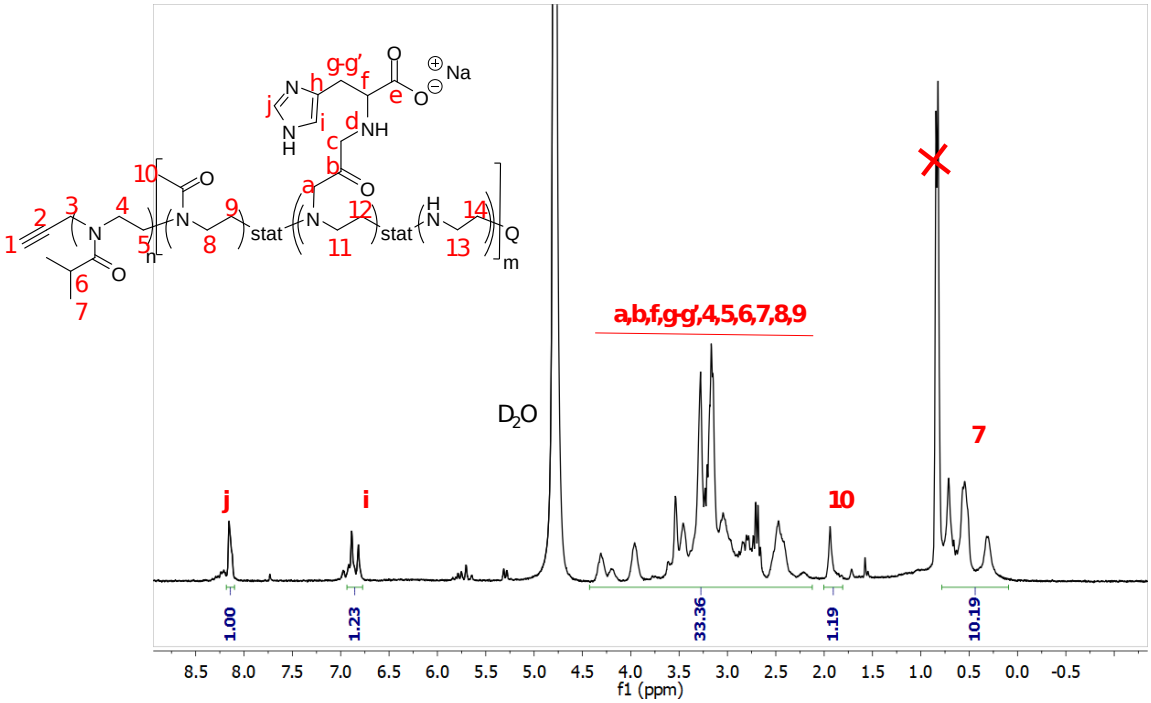

Functionalization calculation:

$$I_{8,6\,ppm} \leftrightarrow 1f$$

$$I_{2.5-4.7\,ppm} - \frac{I(H_7)}{6} \times 5 - \frac{I(H_{10})}{3} \times 4 \leftrightarrow 4(1-f) + 11f$$

$$Soit\, f = ¿\ \frac{4 \times I_{8,6\,ppm}}{I_{2.5-4.7\,ppm} - \frac{I(H_7)}{6} \times 5 - \frac{I(H_{10})}{3} \times 4 - 7 \times I_{8,6\,ppm}}$$

Figure S3 : Cryotransmission electron micrographs of complexes with copolymer C2.

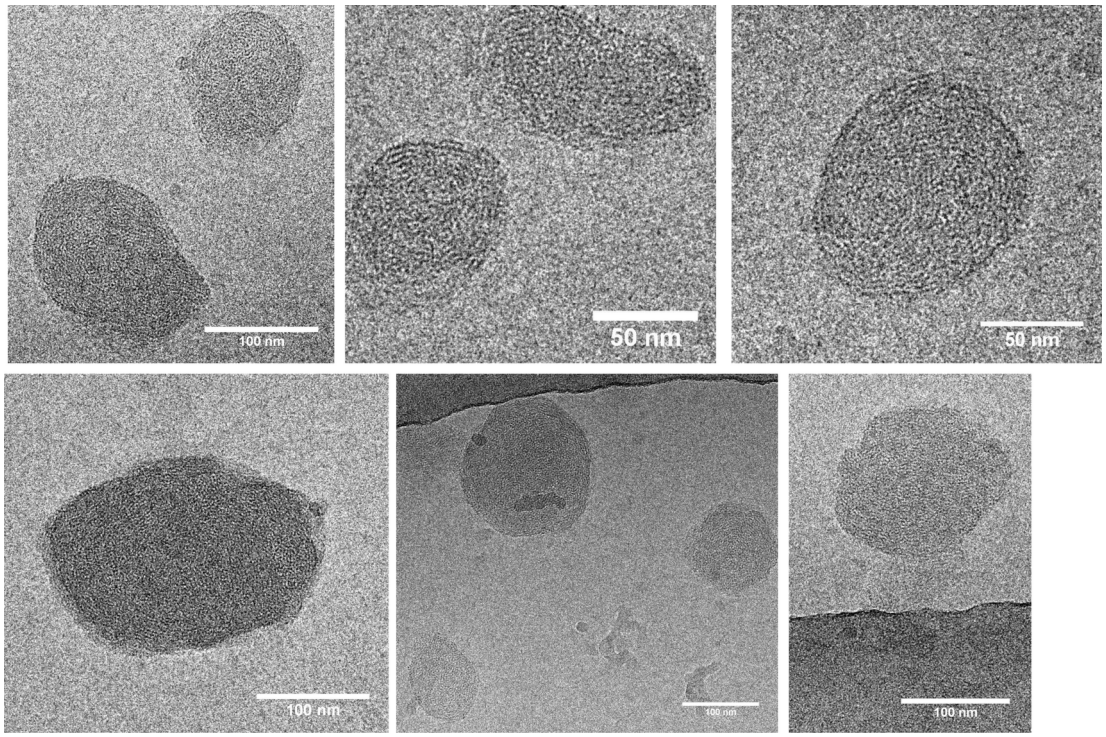

Figure S4: Quantification of the pDNA release with ImageJ

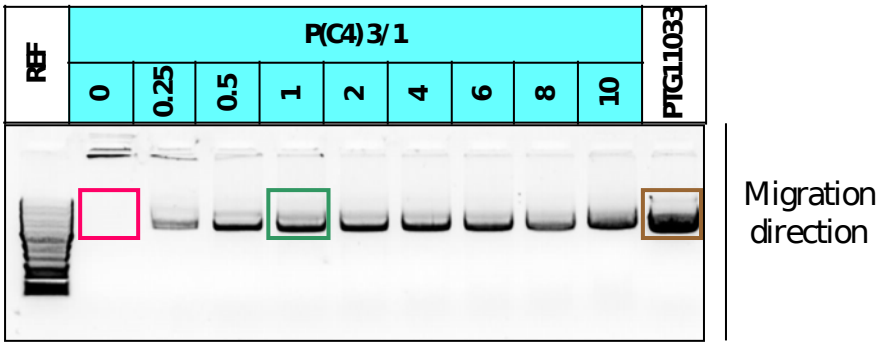

0 to 10 : [dextran sulfate] in $mg.mL^{-1}$

$$\%\ released\ p\ DNA_{1\,\mu g.mL^{-1}} = ¿\ \frac{Mean\,grey\,value_{1\,mg.mL^{-1}} - Mean\,grey\,value_{0\,mg.mL^{-1}}}{Mean\,grey\,value_{p\,DNA} - Mean\,grey\,value_{0\,mg.mL^{-1}}} \times 100$$

Table S1: Formulation parameters with (a) *l*PEI (Px) and (b) PEI-based polymers (Px-his, Cx, Cx-his)

a)

$WR_{polymer}$ = WR_{PEI}	DNA solution		Polymer solution		Total volume (µL)
	V_{DNA} (1 $mg.mL^{-1}$) (µL)	V_{Hepes} (µL)	$V_{polymer}$ (1 $mg.mL^{-1}$) (µL)	V_{Hepes} (µL)	
1/1	10	10	10	10	40
3/1	10	50	30	30	120
5/1	10	90	50	50	200
6/1	10	110	60	60	240
8/1	10	150	80	80	320

$WR_{polymer} = WR_{PEI}$ = (mass of polymer) / (mass of DNA)

b)

WR_{PEI}	**DNA solution**		**Polymer solution**		**Total volume (µL)**
	V_{DNA} (1 mg.mL^{-1}) (µL)	**V_{Hepes}** (µL)	**$V_{polymer}$** (1 mg.mL^{-1}) (µL)	**V_{Hepes}** (µL)	
1/1	10	10	10 / %PEI	20 – $V_{polymer}$	40
3/1	10	50	30 / %PEI	60 – $V_{polymer}$	120
5/1	10	90	50 / %PEI	100 – $V_{polymer}$	200
6/1	10	110	60 / %PEI	120 – $V_{polymer}$	240
8/1	10	150	80 / %PEI	160 – $V_{polymer}$	320

WR_{PEI} = (mass of polymer) × (%PEI) / (mass of DNA) = $WR_{polymer}$ × (%PEI) with %PEI= $M_{n\ PEI\ th}/M_{n\ polymer}$

Calculation of $M_{n\ polymer}$:

For Cx: $M_{n\ polymer} = M_{n\ PEI} + M_{n\ PiPrOx}$

For Px-his: $M_{n\ polymer} = M_{n\ PEI} + DP_{n\ PEI} \times$ %EI modified $\times M_{HNA}$

For Cx-his: $M_{n\ polymer} = M_{n\ PEI} + DP_{n\ PEI} \times$ %EI modified $\times M_{HNA} + M_{n\ PiPrOx}$